Springer

Journal of Mechanical Science and Technology 23 (2009) 195~203

Journal of Mechanical Science and Technology

www.springerlink.com/content/1738-494x
DOI 10.1007/s12206-008-0821-y

Transfer alignment considering measurement time delay and ship body flexure †

Lyou Joon[1,*] and Lim You-Chol[2]

[1]*Department of Electronics Engineering, Chungnam National University, Daejeon, 305-764, Korea*
[2]*Electronics Department, Korea Aerospace Research Institute, Daejeon, 305-33, Korea*

(Manuscript Received March 4, 2008; Revised August 20, 2008; Accepted August 20, 2008)

Abstract

This paper deals with the transfer alignment problem of strap-down inertial navigation systems (SDINS), using electro-magnetic (EM) log velocity information and gyrocompass attitude information of the ship. Major error sources for velocity and attitude matching are lever-arm effect, measurement time-delay, and ship-body flexure (flexibility). To reduce these alignment errors, an error compensation method based on delay state augmentation and DCM (direction cosine matrix) partial matching is devised. A linearized error model for a velocity and attitude matching transfer alignment system is devised by first linearizing the nonlinear measurement equation with respect to its time delay, and augmenting the delay state into conventional linear state equations. DCM partial matching is then properly combined with velocity matching to reduce the effects of a ship's Y-axis flexure. The simulation results show that this method decreases azimuth alignment errors considerably.

Keywords: Kalman filter; Measurement time-delay; Ship body flexure; SDINS; Transfer alignment

1. Introduction

Transfer alignment enables a launched slave inertial navigation system (SINS) to align by using accurate information from the master inertial navigation system (MINS) of a vehicle. The transfer alignment techniques are methodologically divided into angular rate, acceleration, velocity and attitude matching methods [1]. The Kalman filter estimates attitude errors of SINS or mounted misalign between MINS and SINS in the transfer alignment. As the Kalman filter acts like an observer, attitude error estimation is closely related to the observability of the transfer alignment systems. The acceleration or velocity matching method can achieve its alignment goal in horizontal linear accelerated motion, as the angular rate or attitude matching method can in horizontal angular motion. A transfer alignment system based on combined matching methods can optimize the Kalman filter to outperform all others in arbitrary motions. The best combined matching scheme is known to be the velocity and attitude, or angular rate and acceleration, observational method [1-3].

This paper presents a transfer alignment algorithm of the launched SDINS (SINS) EM log and Gyrocompass (MINS) information of the ship, as displayed in Fig. 1. Major error sources for velocity and attitude matching are data-transfer time-delay, ship-body flexure and lever-arm velocity. Lever-arm effect can be easily compensated, as the lever-arm length between MINS and SINS is given. The attitude measurement from the gyrocompass is actually delayed, and this delay is the primary cause of azimuth errors induced during ship motion. Also, a ship's flexure (especially the Y-axis component) is affected at such levels that the mounted misalign between SINS and

† This paper was recommended for publication in revised form by Associate Editor Kyongsu Yi
*Corresponding author. Tel.: +82 42 821 5669
E-mail address: jlyou@cnu.ac.kr

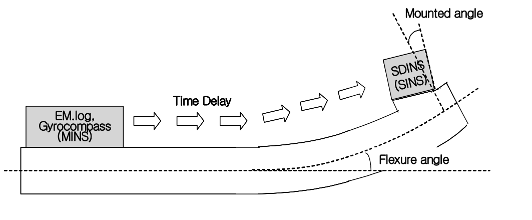

Fig. 1. The concept of transfer alignment including time delay and ship body flexure.

MINS can no longer be regarded as a random constant. Based on this knowledge, this study seeks to reduce alignment errors induced by measurement time-delay and ship-body flexure; to do so, an error compensation method is devised based on delay state augmentation and DCM partial matching.

The paper is organized as follows. In section 2, the Kalman filter model for velocity and attitude matching transfer alignment system is given. Section 3 describes the measurement time-delay error compensation method via delay-state augmentation, and section 4 explains how the DCM partial matching method compensates for some flexure effects. In section 5, to show the validity of the proposed scheme, simulation conditions and results are given. Section 6 contains concluding remarks.

2. Transfer alignment system model

Fig. 2 shows a block diagram of the transfer alignment system constructed by combining EM log velocity matching and gyrocompass attitude matching. The velocity information measured from EM log v_{em} is transformed into the navigation frame by using the DCM $\hat{C}_m^n$, and is subtracted from the estimated velocity of SDINS, $\hat{v}^n$. Then the velocity difference $Z_v = \hat{v}^n - \hat{C}_m^n v_{em}$ is fed into the Kalman filter as a measurement input. On the other hand, the attitude information measured from the gyrocompass, that is, the Euler angle (ϕ, θ, η), is converted into the DCM $\hat{C}_m^n$ and is postmultiplied by the DCM product, $\hat{C}_s^m \hat{C}_n^s$, where $\hat{C}_s^n$ is the DCM of SDINS, and $\hat{C}_s^m$ corresponds to the mounted misalign between MINS and SINS. Also, the attitude error vector Z_{dcm}, or the skew-symmetric matrix of Z_{dcm}, $Z_{dcm} = \hat{C}_m^n \hat{C}_s^m \hat{C}_n^s$ is supplied to the Kalman filter as a measurement input.

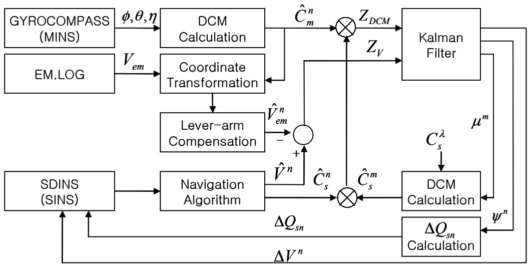

Fig. 2. Transfer alignment system based on EM log velocity and gyrocompass attitude matching.

The model for the design of the Kalman filter for the velocity and attitude matching transfer alignment system is basically given by the velocity error and attitude error differential (state) equations of SDINS [4, 5]. The mounted misalign vector μ is also included in the state equation as a random constant. The measurement vectors, Z_v and Z_{dcm}, described in the previous section are updated in a discrete manner and comprise the measurement equations.

Summarizing the Kalman filter model, the eight-dimensional state vector is defined as Eq. (1), and the corresponding state equations consist of the velocity error Eq. (2), attitude error Eq. (3), and mounted misalign Eq. (4). Also, the five-dimensional measurement equations are given by Eqs. (5) and (6).

$$X = [\Delta v_N, \Delta v_E, \psi_N, \psi_E, \psi_D, \mu_X, \mu_Y, \mu_Z]^T \tag{1}$$

$$\Delta\dot{v} = -(\hat{\Omega}_{ie}^n + \hat{\Omega}_{in}^n)\Delta v + \hat{f}^n \times \psi + w_f \tag{2}$$

$$\dot{\psi} = -\hat{\Omega}_{in}^n \psi + w_\psi \tag{3}$$

$$\dot{\mu} = 0 \tag{4}$$

$$Z_v(k) = \Delta v^n(k) + w_v(k) \tag{5}$$

$$Z_{dcm}(k) = \psi(k) - C_m^n(k)\mu(k) - w_\varepsilon(k) \tag{6}$$

where accelerometer error elements w_f, gyro error elements w_ψ, velocity measurement error elements w_v, and attitude measurement error elements w_ε are assumed to be white noises.

Major error sources of transfer alignment by combining EM log velocity matching and gyrocompass attitude matching are known to be data-transfer time-delay, ship body flexure and lever-arm velocity. The attitude measurement from the gyrocompass is actually delayed, and in turn this principally induces an azimuth error during the ship motion. Also, a ship's flexure affects in such levels that the mounted misalign between SDINS and gyrocompass cannot be regarded as a random constant any longer. Motivated by these, in this study, to reduce alignment errors induced by measurement time-delay and ship body flexure, an error compensation method is devised based on delay state augmentation and DCM partial matching, and is described as follows.

3. Delay-state augmentation

The navigation computer of SDINS receives the delayed attitude information $C_m^n(k-\Delta t)$ and the delayed velocity information $V_{em}(k-\Delta t)$ from gyrocompass and EM log at current time k by the transfer time-delay Δt. The delayed measurement from the gyrocompass and EM log is mismatched with that of SDINS in the time domain. In the case of ship navigation, the instantaneous linear velocity varies much slower than attitude change, and the measurement time-delay effect of the EM log can be neglected compared to that of the gyrocompass. In this respect, the horizontal (N- and E-axes) alignment via velocity matching can be accomplished in spite of the time mismatch, while the performance of the azimuth (D-axis) alignment via attitude matching is degraded. In order to reduce azimuth alignment errors induced by the delayed attitude measurement, we suggest an error compensation method based on the following delay-state augmentation. Let $\hat{C}_m^n(k-\Delta t)$ or $\hat{C}_n^m(\tilde{\phi},\tilde{\theta},\tilde{\eta})$ be the computed DCM matrix using the delayed gyrocompass measurements $(\tilde{\varphi},\tilde{\theta},\tilde{\eta})$, where $\tilde{\phi}=\phi-\Delta\phi$, $\tilde{\theta}=\theta-\Delta\theta$ and $\tilde{\eta}=\eta-\Delta\eta$ are the Euler angles at $k-\Delta t$ (Δt to the current time k).

$$\hat{C}_n^m(\tilde{\phi},\tilde{\theta},\tilde{\eta}) = \begin{bmatrix} \cos\tilde{\theta}\cos\tilde{\eta} & \sin\tilde{\phi}\sin\tilde{\theta}\cos\tilde{\eta} - \cos\tilde{\phi}\sin\tilde{\eta} & \cos\tilde{\phi}\sin\tilde{\theta}\cos\tilde{\eta} + \sin\tilde{\phi}\sin\tilde{\eta} \\ \cos\tilde{\theta}\sin\tilde{\eta} & \sin\tilde{\phi}\sin\tilde{\theta}\sin\tilde{\eta} + \cos\tilde{\phi}\cos\tilde{\eta} & \cos\tilde{\phi}\sin\tilde{\theta}\sin\tilde{\eta} - \sin\tilde{\phi}\cos\tilde{\eta} \\ -\sin\tilde{\theta} & \sin\tilde{\phi}\cos\tilde{\theta} & \cos\tilde{\phi}\cos\tilde{\theta} \end{bmatrix} \tag{7}$$

Since $\Delta\phi$ is small enough, the terms $\sin(\phi+\Delta\phi)$ and $\cos(\phi+\Delta\phi)$ in Eq. (7) can be approximated as:

$$\sin(\phi+\Delta\phi) \approx \sin\phi - \Delta\phi\cos\phi$$
$$\cos(\phi+\Delta\phi) \approx \cos\phi + \Delta\phi\sin\phi$$

which is similar to the cases of $(\theta-\Delta\theta)$ and $(\eta-\Delta\eta)$. Then, using these approximations, $\hat{C}_m^n(\tilde{\phi},\tilde{\theta},\tilde{\eta})$ is divided into two parts:

$$\hat{C}_m^n(\tilde{\phi},\tilde{\theta},\tilde{\eta}) = \hat{C}_m^n(\phi,\theta,\eta) + \Delta\hat{C}_m^n(\Delta\phi,\Delta\theta,\Delta\eta) \tag{8}$$

where

$$\Delta\hat{C}_m^n(\Delta\phi,\Delta\theta,\Delta\eta) = \begin{bmatrix} \Delta\theta\sin\theta\cos\phi + \Delta\eta\cos\theta\sin\eta & -\Delta\phi\cos\phi\sin\theta\cos\eta - \Delta\theta\sin\phi\cos\theta\cos\eta + \Delta\psi\sin\phi\sin\theta\sin\eta - \Delta\phi\sin\phi\sin\eta + \Delta\eta\cos\phi\cos\eta & \Delta\phi\sin\phi\sin\theta\cos\eta - \Delta\theta\cos\phi\cos\vartheta\cos\eta + \Delta\psi\cos\psi\sin\theta\sin\eta + \Delta\phi\cos\phi\sin\eta + \Delta\eta\sin\phi\cos\eta \\ \Delta\theta\sin\theta\sin\eta - \Delta\eta\cos\theta\cos\eta & -\Delta\phi\cos\phi\sin\theta\sin\eta - \Delta\theta\sin\phi\cos\theta\sin\eta - \Delta\eta\sin\phi\sin\theta\cos\eta + \Delta\phi\sin\phi\cos\eta + \Delta\eta\cos\phi\sin\eta & \Delta\phi\sin\phi\sin\theta\sin\eta - \Delta\theta\cos\phi\cos\theta\sin\eta - \Delta\eta\cos\phi\sin\theta\cos\eta + \Delta\phi\cos\phi\cos\eta - \Delta\eta\sin\phi\sin\eta \\ \Delta\theta\cos\theta & -\Delta\phi\cos\phi\cos\theta + \Delta\theta\sin\phi\sin\theta & \Delta\phi\sin\phi\cos\theta + \Delta\theta\cos\phi\sin\theta \end{bmatrix} \tag{9}$$

Again, Eq. (8) can be expressed explicitly in time variable as

$$\hat{C}_m^n(k-\Delta t) = \hat{C}_m^n(k) + \Delta\hat{C}_m^n(k)\Delta t \tag{10}$$

where $\Delta\hat{C}_m^n(k)$ is $\Delta\hat{C}_m^n(\dot{\phi},\dot{\theta},\dot{\eta})$ of Eq. (9) in which $(\Delta\phi,\Delta\theta,\Delta\eta)$ are replaced by $(\dot{\phi},\dot{\theta},\dot{\eta})$. Note that in deriving Eq. (10), other approximations, $\Delta\phi=\dot{\phi}\Delta t$, $\Delta\theta=\dot{\theta}\Delta t$, and $\Delta\psi=\dot{\psi}\Delta t$, are utilized.

Now, subject to the data transport time delay, the attitude measurement equation becomes

$$\begin{aligned} \tilde{Z}_{DCM}(k) &= \hat{C}_m^n(k-\Delta t)\hat{C}_s^m(k)\hat{C}_n^s(k) \\ &= Z_{DCM}(k) + D(k)\Delta t \end{aligned} \tag{11}$$

or in vector form

$$\tilde{Z}_{dcm}(k) = Z_{dcm}(k) + d(k)\Delta t \tag{12}$$

where

$$D(k) = \Delta\hat{C}_m^n(k)\hat{C}_s^m(k)\hat{C}_n^s(k) \tag{13}$$

$$d = [-D_{(2,3)}, D_{(1,3)}, -D_{(1,2)}]^T, \tag{14}$$

and $D_{(i,j)}$ is the element in row i and column j of the matrix D.

As can be seen from Eq. (11), the original measurement equation is linearized with respect to the delay Δt. Furthermore, assuming that Δt is an almost random constant (actually, it has a slow time-varying bias), we can get the augmented model by appending

$$\Delta\dot{t} = 0 \tag{15}$$

into the linear state Eqs. (2)-(4).

For the measurement time delay error compensation to be effective, the delay state Δt needs to be estimated through the Kalman filter. Let us check if the augmented Kalman filter model is observable:

$$X = [\Delta v_N, \Delta v_E, \psi_N, \psi_E, \psi_D, \mu_X, \mu_Y, \mu_Z, \Delta t]^T \tag{16}$$

$$A = \begin{bmatrix} -[\widetilde{\Omega}^n_{ie} + \widetilde{\Omega}^n_{in}] & \widetilde{F}^n & 0_{2\times3} & 0_{2\times1} \\ 0_{3\times2} & -\Omega^n_{in} & 0_{3\times3} & 0_{3\times1} \\ 0_{3\times2} & 0_{3\times3} & 0_{3\times3} & 0_{3\times1} \\ 0_{1\times2} & 0_{1\times3} & 0_{1\times3} & 0_{1\times1} \end{bmatrix} \tag{17}$$

$$H = \begin{bmatrix} I_{2\times2} & 0_{2\times3} & 0_{2\times3} & 0_{2\times1} \\ 0_{3\times2} & I_{3\times3} & -C^n_m & d \end{bmatrix} \tag{18}$$

where the matrix H is time-varying along ship motion conditions. Note that the observability analysis of a time-varying system is quite cumbersome and involves the evaluation of Grammian observability. Hence, instead of this, we apply the observability analysis method for piecewise constant systems [8]. Since in normal weather conditions, the ship moves vary slowly, relative to the measurement sampling frequency as observed in the simulation (see section 5), H in Eq. (18) can be regarded as a continuation of piecewise constant matrices.

Without any ship angle motion, C^n_m and d in Eq. (18) are constant matrices so that $C^n_m = I_{3\times3}$, $d = 0_{3\times1}$, and $\Omega^n_{in} \approx 0_{3\times3}$. The observable states are Δv_N, Δv_E, ψ_N, ψ_E, μ_X, μ_Y, $\psi_D + \mu_Z$ and the time-delay state is not observable.

When there is roll (or pitch) angle motion, it follows that

$$C^n_m = \begin{bmatrix} -1 & 0 & 0 \\ 0 & -\cos\varphi & \sin\varphi \\ 0 & -\sin\varphi & -\cos\varphi \end{bmatrix}, \quad d = \begin{bmatrix} -D_{23} \\ 0 \\ 0 \end{bmatrix}$$

Since C^n_m and d are no longer constant matrices under roll angle motion, all the states in Eq. (16) are shown to be observable and the time-delay state can be estimated based on the observability analysis procedure of [8].

4. DCM partial matching

A ship undergoes roll, pitch, and yaw motions due to waves or windy conditions, and the ship's body flexure in real conditions may cause a time-varying angular rotation of the SDINS axes relative to the gyrocompass. The result is that the mounted misalign μ in Eq. (4) cannot be regarded as a random constant any longer [3, 7].

$$\dot{\mu} = \left[I + \frac{1}{2}M + (1 - \mu_0 \frac{\sin\mu_0}{2(1-\cos\mu_0)})M^2 \right] \omega^s_{ms} \tag{19}$$

where M is the skew-symmetric matrix of μ, μ_0 is the magnitude of μ, and ω^s_{ms} represents the relative angular velocity vector between SDINS and gyrocompass. Note that if the ship's body is rigid, ω^s_{ms} in Eq. (19) becomes zero leading to Eq. (4). Similar to the case of measurement time-delay, this ship-body flexure also induces azimuth alignment errors.

Due to difficulties in modeling the flexure phenomena, there have been few approaches able to compensate for significant flexure effects. In this work, pointing out that the Y-axis flexure component is relatively large and has a significant influence on the Kalman filter's performance of azimuth error estimation, we suggest the so-called "DCM partial matching" method, which excludes the state and measurement variables closely related with Y-axis flexure effects.

To be specific, if μ in Eq. (19) is small enough (within 3°), the terms M and μ_0 can be approximated as $M \approx 0_{3\times3}$ and $\mu_0 \approx 0$, and it becomes

$$\dot{\mu} = \begin{bmatrix} \dot{\mu}_X \\ \dot{\mu}_Y \\ \dot{\mu}_Z \end{bmatrix} \approx \begin{bmatrix} 1 & 0 & 0 \\ 0 & 1 & 0 \\ 0 & 0 & 1 \end{bmatrix} \begin{bmatrix} \omega_{Xx} \\ \omega_{Yy} \\ \omega_{Zz} \end{bmatrix} \tag{20}$$

where $\omega^s_{ms} = [\omega_{Xx}, \omega_{Yy}, \omega_{Zz}]^T$.

From Eq. (20), we see that μ_Y is directly dependent on ω_{Yy}, which is induced by the Y-axis' flexure. Thus, to decouple the alignment errors from the effects of ω_{Yy}, we have only to exclude μ_Y from the error state Eqs. (1) to (4). One remaining problem is how to separate μ_Y from the attitude measurement Eq. (6). Transforming both sides of Eq. (6) by C_n^m, we get

$$\begin{bmatrix}\bar{z}_{dcm(Xx)}\\ \bar{z}_{dcm(Yy)}\\ \bar{z}_{dcm(Zz)}\end{bmatrix} = C_n^m \begin{bmatrix}\psi_N\\ \psi_E\\ \psi_D\end{bmatrix} - \begin{bmatrix}\mu_X\\ \mu_Y\\ \mu_Z\end{bmatrix} + C_n^m d\Delta t - \tilde{w}_\varepsilon \qquad (21)$$

Note that $\bar{z}_{dcm(Yy)}$ in Eq. (21) is dependent on μ_Y only.

In summary, our partial matching scheme is derived by excluding μ_Y and $\bar{z}_{dcm(Yy)}$ from the Eqs. (1) to (6), and the augmented Kalman filter model is given by

$$X = [\Delta v_N, \Delta v_E, \psi_N, \psi_E, \psi_D, \mu_X, \mu_Z, \Delta t]^T \qquad (22)$$

$$A = \begin{bmatrix} -[\tilde{\Omega}_{ie}^n + \tilde{\Omega}_{in}^n] & \tilde{F}^n & 0_{2\times2} & 0_{2\times1} \\ 0_{3\times2} & -\Omega_{in}^n & 0_{3\times2} & 0_{3\times1} \\ 0_{2\times2} & 0_{2\times3} & 0_{2\times2} & 0_{2\times1} \\ 0_{1\times2} & 0_{1\times3} & 0_{1\times2} & 0_{1\times1} \end{bmatrix} \qquad (23)$$

$$H = \begin{bmatrix} 1 & 0 & 0 & 0 & 0 & 0 & 0 & 0 \\ 0 & 1 & 0 & 0 & 0 & 0 & 0 & 0 \\ 0 & 0 & C_{n11}^m & C_{n12}^m & C_{n13}^m & -1 & 0 & -\bar{D}_{23} \\ 0 & 0 & C_{n31}^m & C_{n32}^m & C_{n33}^m & 0 & -1 & -\bar{D}_{12} \end{bmatrix} \qquad (24)$$

In Eq. (22), although μ_Y is excluded in the partial matching, μ_Y can be recovered as follows:

$$\begin{bmatrix}\hat{\mu}_X(k)\\ \hat{\mu}_Y(k)\\ \hat{\mu}_Z(k)\end{bmatrix} = rot\left\{\hat{C}_n^m(k)\hat{C}_s^n(k)\hat{C}_m^s(k-1)\right\} \qquad (25)$$

by using the previous mount misalign information, $\hat{C}_m^s(k-1)$, where 'rot' stands for the rotation vector from DCM. It is also noted that $\hat{C}_n^m(k)$ in Eq. (25) contains undelayed Gyrocompass attitude information that can be advanced by the estimated delay amount.

5. Simulation results

There are many error sources affecting the transfer alignment system. These error sources are classified as either sensor errors or matching errors. Sensor errors are those of SDINS (gyro and accelerometer), EM log, and gyrocompass, while matching errors

Table 1. Frequency and amplitude of the ship's roll and pitch angle motion.

	Frequency (f_i)	Amplitude (A_i)
Roll	0.07 ~ 0.18 Hz	0.42 ~ 2.10°
Pitch	0.11 ~ 0.22 Hz	0.3 ~ 1.5°

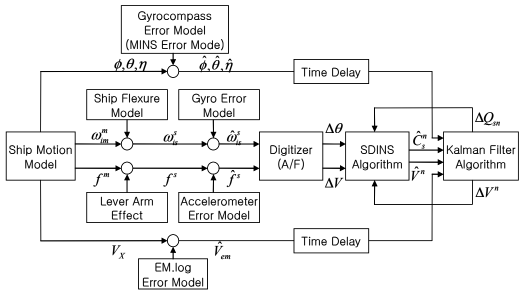

Fig. 3. Computer simulation diagram.

stem from launcher angle, lever-arm effect, sea current, measurement time-delay, and ship-body flexure. Therefore, for a rigorous performance analysis of the transfer alignment algorithm of mixed EM log velocity and gyrocompass attitude matching, all of the above-mentioned error sources should be accounted for, as shown in Fig. 3.

First, ship motion is generated by a combination of sinusoidal waves:

$$\sum_{i=0}^{n} A_i \sin(2\pi f_i t + p_i), \quad 0 < p_i < 2\pi \qquad (26)$$

where A_i and f_i are the amplitude and the frequency of the ith harmonic, respectively. For simplicity, only roll and pitch motions are treated in the simulations, and according to the usual frequency spectrum [9, 10], the corresponding A_i and f_i are assigned as in Table 1. Also, the sensor errors of SDINS are modeled by Eqs. (27) and (28), and their magnitudes are specified in Table 2.

[Gyro error model]

$$\delta\omega = \delta\varpi_B + \delta K_g \omega_{ib}^b + \Delta N_g \omega_{ib}^b + \Delta M_g a^b + \delta E_g a^b + \delta C_g \tilde{\omega}_c^b + \delta I_g \tilde{\omega}_g^b + \delta\Omega_g \dot{\omega}_g + g_{white} + g_{walk} + g_{markov} \qquad (27)$$

[Accelerometer error model]

$$\delta f = \delta a_B + \delta K_a a^b + \Delta N_a a^b + \delta I_a \tilde{\omega}_a^b + \delta\Omega_a \dot{\omega}_a + a_{white} + a_{walk} + a_{markov} \qquad (28)$$

Table 2. Sensor error elements of SDINS.

Gyro	Magnitude : 1σ	
Bias repeatability	0.2 deg/hr	$\delta\varpi_B$
Scale factor stability	200 ppm	δK_g
Misalign	1.0 arcmin	ΔN_g
Mass-unbalance	0.05 deg/hr/g	ΔM_g
Anisoelastic	0.5 deg/hr/g^2	δE_g
Anisoinertia	0.5 deg/deg/ (rad/sec)^2	δI_g
Cross-coupling	0.5 deg/deg/ (rad/sec)^2	δC_g
Angle-rate sensitivity	0.5 deg/deg/ (rad/sec)^2	$\delta\Omega_g$
White noise	0.01 deg/hr	g_{white}
Random walk	0.001 deg/hr/hr$^{1/2}$	g_{walk}
1st markov	0.05 deg/hr , 1.0 min	g_{markov}

Accelerometer	Magnitude : 1σ	
Bias repeatability	200 μg	δa_B
Scale factor stability	200 ppm	δK_a
Misalign	1.0 arcmin	ΔN_a
Anisoinertia	50 μg/ (rad/sec)^2	δI_a
Angle-rate sensitivity	50 μg/ (rad/sec)^2	$\delta\Omega_a$
White noise	40 μg	a_{white}
Random walk	10 μg/ hr$^{1/2}$	a_{walk}
1st markov	30 μg , 1.0 min	a_{markov}

Next, the sensor information from gyrocompass and EM log is generated by Eqs. (29) and (30), and the magnitude of sensor errors is given in Tables 3 and 4.

$$\hat{\varphi} = \tan^{-1}\left[\frac{-\delta P_n \cos\psi - \delta P_e \sin\psi}{\cos\theta - \sin\theta(\delta P_n \sin\psi - \delta P \cos\psi)}\right] + \delta S_\varphi \sin 2\varphi + \delta N_\varphi \quad (29a)$$

$$\hat{\theta} = \sin^{-1}\left[\sin\theta + \cos\theta(\delta P_n \sin\psi - \delta P_e \cos\psi)\right] + \delta S_\theta \sin 2\theta + \delta N_\theta \cos\varphi \quad (29b)$$

$$\hat{\psi} = \tan^{-1}\left[\frac{\cos\theta \sin(\psi + \delta P_d) - \delta P_n \sin\theta}{\cos\theta\cos(\psi + \delta P_d) + \delta P_e \sin\theta}\right] + \delta S_\psi \sin 2\psi + \delta N_\psi \frac{\cos\varphi}{\cos\theta} \quad (29c)$$

$$v_{em} = v_X + v_{wX} + a v_Y + \Delta B v_Z + v_{em}\delta K_{em} + \delta v_{em} + w_{em} \quad (30)$$

Table 3. Sensor error elements of the gyrocompass.

	Magnitude : 1σ	
Stable platform tilt	3 arcmin	δP
Synchro-conversion error	5 arcmin	δS
Non-orthogonality	5 arcmin	δN
1st Markov noise	1 arcmin , 0.1 sec	−

Table 4. Sensor error elements of the EM log.

	Magnitude : 1σ	
Sea current	0.5 m/sec	v_w
Probe misalign	1 deg	a
Magnetic field scattering	1 %	ΔB
Bias	0.1 m/sec	δv_{em}
Scale factor stability	1 %	δK_{em}
White noise	0.2 m/sec	w_{em}

Table 5. Ship flexure parameters.

	ω_n	ς	σ
X-axis	0.20 Hz	0.1	0.01°
Y-axis	0.15 Hz	0.5	0.1°
Z-axis	0.25 Hz	0.5	0.001°

Taking into account the actual communication delay between gyrocompass and SDINS, it is assumed that the time-delay may vary within 30 msec and may jump by 5 msec several times, and that ship-body flexure is modeled by the second markov process [6] with a magnitude (1 σ) of 0.001° ~ 0.1° :

$$\ddot{\theta}_f + 2\zeta\omega_n\dot{\theta}_f + \omega_n^2\theta_f = w \quad (31)$$

where w is white noise with $E(w) = 0$ and $E(w^2) = 4\zeta\omega_n^3\sigma^2$, and the corresponding parameters are chosen as shown in Table 5 .

Now, by repeating Monte Carlo simulations, the effects caused by various error sources on the transfer alignment of three axes are evaluated and depicted in the histogram of Fig. 4.

Notations in Fig. 4	
① Launcher angle	② Lever-arm effect
③ Sea current	④ Gyro error
⑤ Accelerometer error	⑥ EM log error
⑦ Gyrocompass error	⑧ Measurement time-delay
⑨ Ship-body flexure	

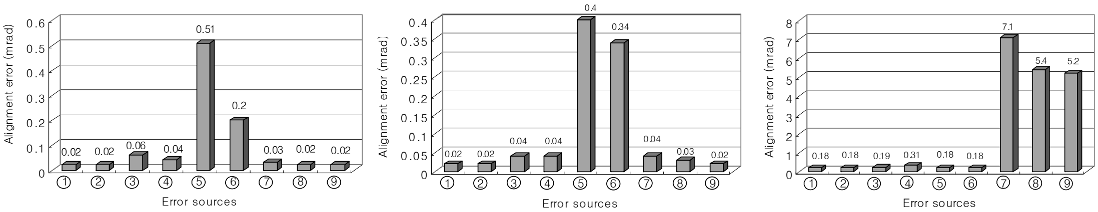

(a) N-axis alignment performance (b) E-axis alignment performance (c) D-axis alignment performance

Fig. 4. Effects by various sources on transfer alignment.

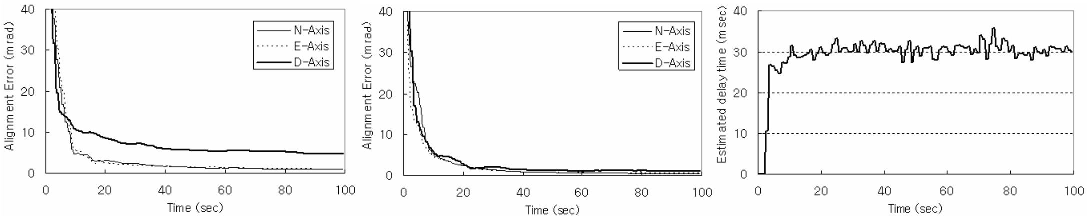

(a) Without compensation (b) With compensation (c) Estimate delay state

Fig. 5. Alignment performance about measurement time-delay.

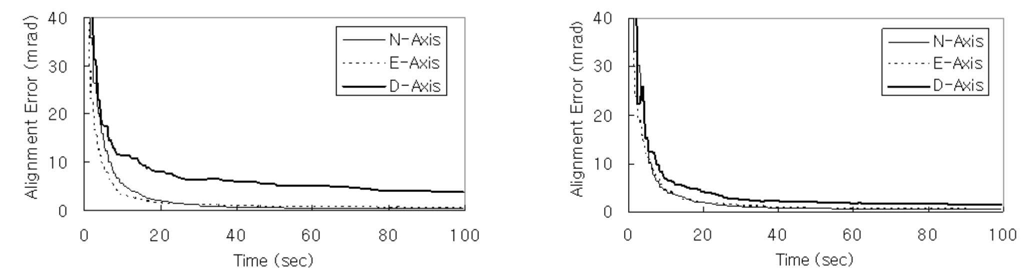

(a) Without compensation (b) With compensation

Fig. 6. Alignment performance about ship body flexure.

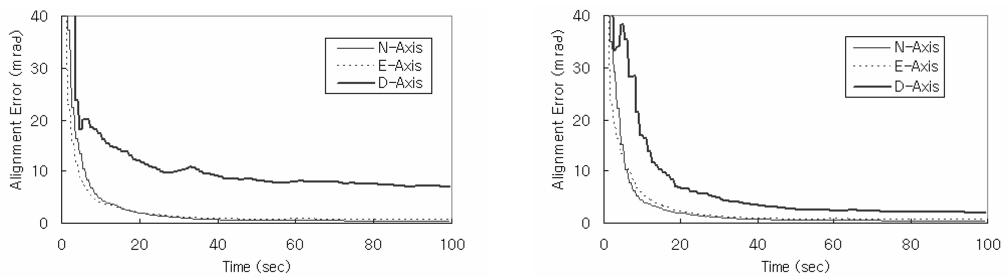

(a) Without compensation (b) With compensation

Fig. 7. Alignment performance about measurement time-delay and ship body flexure.

From the figures, notice that the error range of the D-axis is at least 10 times wider than the error range of the other axes, which means that the azimuth alignment is degraded significantly. Fig. 4(c) shows that the main error sources are gyrocompass error, measurement time-delay and ship-body flexure. However, in this study, gyrocompass error is not considered and is treated as a sensor error in itself.

Figs. 5-7 show, respectively, Monte Carlo simulation results without and with error compensation using the present method and assuming a worst-case scenario in which the delay continues for 30*msec* and

1σ of Y-axis's flexure is 0.1°. Note that the delay amount and flexure magnitude are assumed to be known only for simulation purposes. Comparing the two figures with and without compensation, the augmented Kalman filter with DCM partial matching performs much better in the D-axis alignment than the conventional Kalman filter. To be specific, the azimuth angle error settles down about 2*mrad* in 60 seconds for the present case, while showing about 8*mrad* for the conventional one. As displayed in Fig. 5(c), the delay state can be estimated during ship motions, resulting in considerably less misalignment.

6. Concluding remarks

An error compensation framework for the EM log velocity and gyrocompass attitude matching transfer alignment system has been established through delay state augmentation and DCM partial matching. Through the observability analysis and the interpretation of results from computer simulations, we find that this approach effectively improves azimuth alignment performance. Surprisingly, the errors induced by measurement time-delay and ship-body flexure decrease by 25%.

Nomenclature

i : Inertial frame
e : Earth fixed frame
n : Navigation frame (N,E,D)
s : IMU (Inertial Measurement Unit) frame of SDINS
m : Gyrocompass (ship body) frame (X,Y,Z)
m' : Perturbed m frame by ship body flexure
λ : Launcher frame
C_A^B : Transformation matrix from A frame to B frame
v^A : Velocity coordinated in A frame
f^A : Acceleration coordinated in A frame
ω_{ij}^A : Angular velocity of i frame relative to j frame, coordinated in A frame
Ω_{ij}^A : Skew-symmetric form of ω_{ij}^A
F^A : Skew-symmetric form of f^A
$(\hat{\ })$: Computed value
μ : Mounted misalign error between SDINS and gyrocompass
Δv : SDINS velocity error
ψ : SDINS attitude error

References

[1] K. Spalding, An Efficient Rapid Transfer Alignment Filter, *Proc. of the AIAA GN&C Conference*, (1992) 1276-1286.
[2] J. E. Kain, J. R. Cloutier, Rapid Transfer Alignment for Transfer Weapon Application, *Proc. of the AIAA GN&C Conference*, (1989) 1290-1300.
[3] A. M. Schneider, Kalman Filter Formulations for Transfer Alignment of Strapdown Inertial Units, *Journal of the Institute of Navigation*, 30 (1) (1983) 72-89.
[4] G. M. Siouris, *Aerospace Avionics Systems: A Modern Synthesis,* Academic Press (1993).
[5] K. R. Britting, *InertialNavigation Systems Analysis,* Wiley & Sons (1971).
[6] D. H. Titteron and J. L. Westone, Dynamic Shipboard Alignment Technique, *Symposium Gyro Technology*, *(*1989) 9.1-9.27.
[7] N. M. Vepa, A Dynamic Alignment System for Applications on Flexible Platforms such as Ships, *Gyro Technology*, *(*1989) 16.1-16.3.
[8] D. Goshen-Meskin and I. Y. Bar-Itzhack, Observability Analysis of Piece-Wise Constant System, Part I: 'Theory' & Part II: 'Application to Inertial Navigation In-Flight Alignment, *IEEE Trans. On AES.*, 28 (4) (1992) 1056-1075.
[9] P. J. Gates and N. M. Lynn, *Ships, Submarines and the Sea*, Brassey's (UK), London (1990).
[10] K. J. Rawson, E.C. Tupper, *Basic Ship Theory*, Longman, London (1968).

Joon Lyou received a B.S. degree in Electronics Engineering from Seoul National University in 1978. He then went on to receive M.S. and Ph.D. degrees from KAIST in 1980 and 1984, respectively. Dr. Lyou is currently a professor of the Department of Electronics Engineering at Chungnam National University in Daejeon, Korea. His research interests include industrial control and sensor signal processing, IT based robotics, and navigation systems.

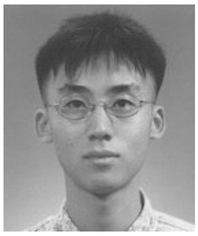

You-Chol Lim received a B.S. degree in Electronics Engineering from Chungnam National University in 1998. He then received his M.S. and Ph.D. degrees from Chungnam National University in 2000 and 2003, respectively. Dr. Lim is currently a senior researcher at Electronics Department KSLV Technology Division at KARI in Daejeon, Korea. Dr. Lim's research interests are in the area of remote control, digital filter, and navigation systems.